NATIONAL ADVISORY COMMITTEE FOR AERONAUTICS

TECHNICAL NOTE 4240

SOME MEASUREMENTS OF AERODYNAMIC FORCES AND MOMENTS AT SUBSONIC SPEEDS ON A RECTANGULAR WING OF ASPECT RATIO 2 OSCILLATING ABOUT THE MIDCHORD

By Edward Widmayer, Jr., Sherman A. Clevenson, and Sumner A. Leadbetter

Langley Aeronautical Laboratory
Langley Field, Va.

Washington
May, 1958

NATIONAL ADVISORY COMMITTEE FOR AERONAUTICS

TECHNICAL NOTE 4240

SOME MEASUREMENTS OF AERODYNAMIC FORCES AND MOMENTS AT SUBSONIC SPEEDS ON A RECTANGULAR WING OF ASPECT RATIO 2 OSCILLATING ABOUT THE MIDCHORD[1]

By Edward Widmayer, Jr., Sherman A. Clevenson, and Sumner A. Leadbetter

SUMMARY

Some measurements were made of the aerodynamic forces and moments acting on a rectangular wing of aspect ratio 2 which was oscillated about the midchord. These measurements were made at four frequencies (31, 43, 54, and 62 cps) over a range of Mach number from 0.15 to 0.81, a range of reduced frequency from 0.15 to 1.32, and a range of Reynolds number from 0.60×10^6 to 9.21×10^6. It was feasible to compare results of a portion of these measurements with some published experimental data and, in general, reasonable agreement was found to exist. An appendix is included to show the correction of the root reaction for inertia and aerodynamic effects in order to determine the total aerodynamic load.

Comparison of the measured aerodynamic forces and moments with those predicted by the method of Reissner and by the method of Lawrence and Gerber for wings of aspect ratio 2 in incompressible flow showed generally good agreement. Comparison of the measured quantities with those predicted by two-dimensional-flow theory indicated that the effects of finiteness of span on the aerodynamic forces and moments are considerable. Some experimental results pertaining to the influence of wind-tunnel-wall effects on nonsteady aerodynamic measurement have been included.

INTRODUCTION

A need exists for experimental measurements of oscillating air forces because of the significance of these forces in flutter and related fields, and in order to assess past and present theoretical work. Despite the importance of the problem, only a limited amount of data, both experimental

[1]Supersedes recently declassified Research Memorandum L53F19 by Edward Widmayer, Jr., Sherman A. Clevenson, and Sumner A. Leadbetter, 1953.

and theoretical, exists for restricted ranges of aspect ratio, Mach number, and Reynolds number. (See, for instance, ref. 1.)

Theoretical treatment of aspect-ratio effects on the oscillatory aerodynamic coefficients for subsonic speeds is in a state of development and is not yet in a form convenient for numerical comparison. There is difficulty in mathematically representing the physical phenomena and certain assumptions necessary to obtain a solution are doubtful, particularly those associated with tip effects. Consequently, current experimental measurements will be compared with readily available experimental and theoretical oscillatory coefficients.

This paper presents some experimental measurements of the oscillatory aerodynamic forces and moments acting on a rectangular wing of aspect ratio 2 which was oscillated about the midchord. These coefficients are presented for a range of reduced frequency from 0.15 to 1.32 and for a range of Mach numbers from 0.15 to 0.81. The Reynolds number ranged from 0.60×10^6 to 9.21×10^6. These measurements were made by using a resonant oscillation technique in the Langley 2- by 4-foot flutter research tunnel with air or Freon-12 as a testing medium. A comparison of the measured values has been made with some existing experimental data and with the results of the analyses of references 2 and 3, that is, of Reissner and of Lawrence and Gerber. In order to establish some convenient reference values, coefficients for two-dimensional incompressible flow (ref. 4) are indicated. The results are presented in tabular form for quantitative evaluation and in graphical form for qualitative examination and comparison.

SYMBOLS

A	aspect ratio
a	speed of sound, fps
c	chord of wing, ft
EI	bending stiffness where E is Young's modulus and I is section moment of inertia
g_s	logarithmic damping coefficient of wing in a near vacuum
g_t or λ	logarithmic damping coefficient of wing in airstream
H	tunnel height, ft

I_s effective inertia of oscillating system accounting for dynamic deformation of system, ft-lb-sec^2/radian

K_s effective spring constant of oscillating system, ft-lb/radian

k reduced-frequency parameter, $\omega c/2v$

k_s spring constant of a simple mass-spring system, ft-lb/radian

L oscillating lift vector acting on wing for oscillations about midchord axis, positive when acting downward,

$$|L|e^{i\left(\omega t+\frac{\pi\phi}{180}\right)} = -(\pi\rho v^2 sc|\alpha|)\left(l_1 + il_2\right)e^{i\omega t}$$

l_1 nondimensional coefficient of lift in phase with angular displacement

l_2 nondimensional coefficient of lift in phase with angular velocity

M Mach number

M_α oscillating moment vector acting on wing for oscillation about midchord, referred to the axis of rotation, positive for leading edge up,

$$|M_\alpha|e^{i\left(\omega t+\frac{\pi\theta}{180}\right)} = (\pi/2)\rho v^2 sc^2|\alpha|(m_1 + im_2)e^{i\omega t}$$

m wing mass, slugs

m_1 nondimensional moment coefficient in phase with angular displacement

m_2 nondimensional moment coefficient in phase with angular velocity

R Reynolds number

s semispan of wing, ft

t time, sec

v velocity of test medium, fps

x spanwise coordinate

y deflection coordinate

α angle of incidence at $s/2$ span station as a function of time, $|\alpha|e^{i\omega t}$, radians

θ phase angle between moment vector and incidence vector, $\tan^{-1}(m_2/m_1)$, deg

ρ mass density of test medium, slugs/cu ft

ϕ phase angle between lift vector and incidence vector, $\tan^{-1}(l_2/l_1)$, deg

ω_1 circular frequency of oscillation of wing, radians/sec

ω_h circular frequency of first natural wing bending, radians/sec

ω_{vac} circular frequency of oscillation of wing in a near vacuum, radians/sec

A dot over a symbol indicates a derivative with respect to time.

APPARATUS AND METHOD

Tunnel

The Langley 2- by 4-foot flutter research tunnel was used for the tests reported herein with the test section modified to be rectangular in shape, measuring 45.75 by 24 inches. The test mediums were air and mixtures of air and Freon-12 as noted for each set of data. The use of the air and Freon-12 mixture as a test medium permits the attainment of approximately twice the reduced frequency obtained in air for a given Mach number and frequency. The choking Mach number for these tests was approximately 0.92. The wing was mounted in the test section as shown in figure 1 and with its wall reflection had an aspect ratio of 2.

Wing Model

The semispan wing model had a rectangular plan form with a 12-inch chord and a 12-inch semispan corresponding to an aspect ratio of 2. Fabricated construction was employed; a steel box spar carried four evenly spaced ribs to which plywood skin was attached forming an NACA 65A010 airfoil section. The wing was designed to have high natural

frequencies in order to reduce the amount of correction to the measured forces due to elastic deformations and to bending inertia loads. The first natural cantilever bending frequency ranged from 125 to 130 cps.

The semispan wing model was mounted as a cantilever beam at the tunnel wall in an oscillator mechanism. The mount permitted the wing to oscillate in pitch about the midchord axis. The wing was mass balanced about this axis of oscillation in such a way that there were no lift reactions when the wing was oscillated in a near vacuum.

Oscillating Mechanism

The oscillating mechanism may be considered as a simple torsional vibratory system as illustrated in figure 1. The system consists of a torsion spring which is fixed at one end, a hollow steel shaft which is supported by bearings, and the semispan wing which has a base plate that is flush with the tunnel wall. The mechanism was oscillated in torsion at the natural frequency of the simple spring-inertia system by applying a harmonically varying torque through the shaker coils attached to the shaft. Different springs were used to permit a choice of frequency of oscillation. The springs used and the resulting torsional natural frequencies in a vacuum were as follows:

Spring	ω_{vac}, radians/sec
A	$31 \times 2\pi$
B	43
C	54
D	62

The bearings were contained in housings which were carried on columns. These columns were designed to include stress-sensitive regions and were equipped with strain gages from which the aerodynamic lift could be determined. The vertical reactions at the fixed end of the torsion spring were negligible because of the rigidity of the steel tube and the small deformations experienced by the strain-gage columns.

The electromagnetic shakers consisted of stationary coils furnishing a steady magnetic field and moving coils which were attached to the steel shaft. The moving coils were driven by a variable-frequency oscillator.

The moving coils were alined so that the direction of the applied force was perpendicular to the direction of the lift. Provision was made for interrupting the power to the moving coils in order to obtain a power-off decaying oscillation.

Instrumentation

The instrumentation of the experiment was designed to provide signals that were a measure of the lift and angular position at any instant and to provide a means of measuring their amplitude and time relationship. The lift reactions were converted to electrical signals by means of wire strain gages attached to the supporting columns. The gages were connected so that only lifting loads were sensed. An electrical signal from a wire strain gage mounted on the torsion spring so as to sense torsional strains was calibrated to give the angular displacement in terms of the wing incidence. The signals were filtered and measured with vacuum-tube voltmeters.

The angular-position signal was recorded on a recording oscillograph during the decay of the oscillation for the purpose of obtaining the damping factor. The phase measurements were made with an electronic counter chronograph. The time lapse between a given point on a lift signal and a corresponding point on the position signal was measured while the wing was oscillating at a constant frequency. The period of oscillation was measured with this instrument by determining the time lapse between corresponding points on the same signal.

Calibration

The angular position of the wing was dynamically calibrated with the signal from the torsion strain gages by a photographic technique. Time exposures were taken of a fine chordwise line on the tip of the wing for various amplitudes while the signal output was recorded. The amplitude of oscillation of the wing was obtained from the enveloped position of the line on the wing tip and correlated with the strain-gage signal. By using this procedure and a line on the leading edge, it was determined that, at the maximum frequency of oscillation (62 cps), the tip angle of incidence exceeded the root angle of incidence by less than 2 percent.

The signals from the balance columns were calibrated in terms of pounds of force per unit of signal strength. Known loads were applied to the wing, and the column reactions were determined by treating the wing shaft system as a simple beam with overhang. (See, for instance, fig. 1.) The reaction forces were then related to the respective signals. The meters were calibrated dynamically by using a voltage divider referred to the open-circuit calibration of the strain gages. The vacuum-tube-voltmeter readings are believed to be within ± 4 percent of true signal.

In order to minimize errors in phase angle ϕ introduced in the electrical operations, a tare value of phase angle was obtained at each reading by applying either the lift or incidence signals through both channels of the electrical circuits. The phase-measuring system was calibrated at various frequencies by using standard resistance-capacitance phase-shift circuits and by using a cam-operated set of cantilever beams on which strain gages had been mounted. The latter system had distortion and noise and approximated the worst tunnel condition. Calibrations of the phase meter indicated that the phase angle may be determined within $\pm 3^\circ$ of true value with a noisy signal and within $\pm 0.5^\circ$ of true value with a clean signal.

Data Reduction

The lift forces as received from the balances contain an aerodynamic component and an inertia component which arises from the bending deformation of the wing. In order to correct the measured lift to the aerodynamic lift, it was necessary to correct for the inertia forces due to wing deformation. A discussion of this correction is given in appendix A. The inclusion of this correction leads to a factor which, when multiplied by the measured lift, gives the actual applied lift. Values of the factor are 0.98 for spring A, 0.95 for spring B, 0.91 for spring C, and 0.87 for spring D. In order to estimate the possible error incurred by neglecting the aerodynamic forces and moments arising from the bending deformation, these forces were included in the analysis in appendix A and were found to be less than 1 percent of the correction due to wing deformation caused by the inertia forces. The phase angle ϕ contained a component due to these forces that tended to increase ϕ by less than 1°. The moments due to the bending deflection were found to be negligible relative to the magnitude of the measured moment. As the aerodynamic effects due to wing bending were within the accuracy of the measurement, no effort was made to adjust for these quantities.

The in-phase moment was determined from the change in resonant frequency due to air flowing over the wing as indicated in reference 5. Since the torsional damping was relatively small, its effect on the frequency is neglected and the entire shift is attributed to the in-phase moment. The coefficient of the in-phase moment is given by

$$m_1 = \frac{-K_s}{\frac{\pi}{2}\rho v^2 c^2 s}\left[\left(\frac{\omega_1}{\omega_{vac}}\right)^2 - 1\right]$$

The dependency of m_1 on the small difference of two quantities of the same magnitude leads to considerable loss in accuracy and consequent

scatter in the data. This scatter became so large for the torsional springs C and D that those coefficients are not presented.

The quadrature-moment coefficient was determined by operating on the logarithmic decrement of the power-off decay of the oscillation. The coefficient m_2 was given by

$$-m_2 = \frac{I_s \omega_1^2}{\frac{\pi}{2} \rho v^2 c^2 s} \left[g_t - \left(\frac{\omega_{vac}}{\omega_1} \right)^2 g_s \right]$$

The derivation of this equation is treated in appendix B.

The phase angle θ between the moment vector and the angle of incidence was obtained from the relationship $\theta = \tan^{-1}\left(m_2/m_1\right)$. The lack of precision of determining m_1 and m_2 directly affects the degree of accuracy of θ; the values of θ are not expected to be more accurate than their components.

RESULTS AND DISCUSSION

The experimental results for the measured aerodynamic forces and moments are presented in tables I to IV. These results cover four overlapping ranges of reduced frequency (one range in each table) because the Mach number was varied over a range while the frequency varied only a small amount (due to the change in aerodynamic moment). The measured values of lift and moment coefficients and their respective phase angles are shown in tables I and II, whereas the in-phase moments and moment phase angles are omitted from tables III and IV.

The calculated values of the various theories are given in tables V to VII for convenience of discussion and comparison with experimental coefficients. Some calculated values are also shown in various figures for ease in comparing trends. Experimental data relating to the influence of wind-tunnel walls on the aerodynamic forces and moments are presented in table VIII.

Before presenting the actual coefficients of lift and moment and their respective phase angles, the effect of Mach number and Reynolds number on the coefficients will be briefly mentioned. A comparison of some of the current data will then be made with some other experimentally determined coefficients obtained from another source (ref. 6). Comparisons of the current data with the two aspect-ratio theories will then be made. For reference, coefficients for two-dimensional incompressible flow

will also be shown. The section will be concluded with a brief discussion of wind-tunnel-wall effects.

A study was made to determine the effects of Mach number and Reynolds number on the aerodynamic coefficients. Since the testing technique used did not readily permit either k, M, or R to be held constant while the remaining two parameters are varied, a considerable amount of cross plotting was necessary to obtain any indication of an effect due to Mach number or Reynolds number. Insufficient data were available for this purpose and much extrapolation and interpolation were necessary. In light of the experimental inaccuracies (perhaps of the order of the particular effects sought) and the operations necessary to obtain the results, no quantitative information could be obtained. This study indicated that the aerodynamic coefficient possibly was influenced to some extent by both Reynolds number and Mach number. However, for the ranges of speed and frequency covered in this series of experiments, the overall effects of the Reynolds number and Mach number appear not to be of first order and to lie perhaps within the accuracy of the experiment.

In view of the paucity of experimentally determined oscillatory aerodynamic coefficients for finite wings, it is of interest to compare these data with available data from other sources. Reference 6 has presented experimental data for a rectangular wing having the same aspect ratio and axis of rotation as the wing discussed herein, but for a lower range of Mach number and Reynolds number. It should be remarked that there are differences in techniques; the moment coefficients of reference 6 were obtained for the case of steady oscillation, whereas the moment coefficients of the present paper were obtained from the method of decaying oscillations. However, in reference 5 it was shown that for a two-dimensional wing the damping moment obtained from steady oscillations was in agreement with that obtained from decaying oscillations.

A comparison of the results presented herein with those published in reference 6 is shown in figure 2. It may be seen that, for the magnitudes of the lift and moment, there is good agreement. This agreement is gratifying and, since different methods of measurement were used, the magnitudes shown may be considered valid. Large discrepancies may be noted between moment phase angles. The data of reference 6 fall close to a phase angle of 0° and show some values which indicate negative aerodynamic damping. The reasons for the discrepancy in the moment-phase-angle results between reference 6 and the present paper are not known. A comparison of current moment-phase angles with results of calculations is presented subsequently.

Additional data on the experimental damping-moment coefficients have been given in reference 7. These coefficients were obtained by the method of decaying oscillations for a rectangular wing of aspect ratio 2 with

pitch axis at the midchord. The results of reference 7 are compared with the data of this paper in figure 3, the solid and dashed curves being taken from reference 7 and the symbols representing results from this paper. Despite the differences in Reynolds number, it may be noted that the data from the present investigation are in basic agreement with other published results.

The comparisons of the experimental coefficients and phase angles with the theoretical oscillatory coefficients and phase angles for a finite wing will be made only for the incompressible case in this paper. The results of two theories, namely, those of Reissner (ref. 2) and Lawrence and Gerber (ref. 3), were readily available, whereas coefficients for finite wings in compressible flow were not. In making these comparisons, it is recognized that Reissner limits the applicability of his theory to an aspect ratio of 3. No effort has been made in this paper to evaluate the relative merits of the two theories. In order to illustrate the influence of finiteness of span, further comparisons of the experimental data have been made with the coefficients for a two-dimensional incompressible fluid (ref. 4). These comparisons may be made by referring to figures 4 to 8.

In figure 4 may be seen the coefficient of the magnitude of the lift vector as a function of $1/k$. In this presentation it should be recalled that the data for different torsional springs at a given value of $1/k$ were obtained at different Mach numbers. It may be seen that, for the low values of $1/k$, experimental data fall between the theory of Lawrence and Gerber and the theory of Reissner, whereas for the higher values of $1/k$, the theory of Reissner appears to be in agreement with the data and the theory of Lawrence and Gerber falls below the measured lift coefficients. The higher M values correspond to the higher $1/k$ values. The steady-state lift coefficients corrected for aspect ratio by the factor $\frac{A}{A + 2}$ for the incompressible case and by the factor $\frac{A}{A\sqrt{1 - M^2} + 2}$ as suggested in reference 8 for the compressible case evaluated for $M = 0.70$ also are shown in figure 4. The value of the incompressible approximation to the steady-state lift coefficient is a fair representation of the experimental values for $1/k$ greater than 1.5. The experimental values do not appear to vary appreciably from the value determined by the correction $\frac{A}{A + 2}$. Thus, it might appear that the steady-state lift coefficient could be used as a basis for estimating the magnitude of the lift coefficient over a considerable range of reduced frequency. The inadequacy of estimating these coefficients with two-dimensional incompressible-flow theory with no correction or modification is also indicated in figure 5. This correction would appear to vary for this case from 0.67 for a value of $1/k$ of 2.5 to 0.56 for a value of $1/k$ of 6.0.

The measured phase angle of the lift vector for spring A is compared with theoretical phase angles in figure 5. The theories may be noted to agree in general and the theory of Reissner is in good agreement with the measured values, the theory of Lawrence and Gerber falls above the measured values by a few degrees, and the two-dimensional-flow theory is seen to fall below the measured values by a few degrees. The phase angle as given by the aspect-ratio theories and as measured appears to approximate a linear function of reduced frequency in the range of k from 0.2 to 0.7. Since the frequency was essentially constant for a given torsional spring, the low values of reduced frequency were obtained at the higher values of Mach number. In general, the phase angle of the lift appears to be predicted by the aspect-ratio theories of references 2 and 3.

Although some of the moment coefficients have already been presented as magnitudes and phase angles (fig. 2), the components of the measured moments are compared with the components of the theoretical moments. It is felt that, since the measured values were determined as components, it is appropriate to compare these values with theoretical components. By referring to figure 6 it may be seen for the in-phase moment coefficient that the aspect-ratio theories give values which are in general agreement with the data. The two-dimensional-flow theory is given for reference only. With regard to the values given by the aspect-ratio theories, it is seen that there is little difference between them although the theory of Lawrence and Gerber appears to agree a little better with the measured values. One other comparison that may be made is with the steady-state value of the moment coefficient, for which there is no damping moment. The coefficients with the correction $\frac{A}{A + 2}$ and including compressibility $\frac{A}{A\sqrt{1 - M^2} + 2}$ are indicated in figure 6. It appears that the steady-state coefficient uncorrected for Mach number but corrected for aspect ratio could be used as a basis for estimating the magnitude of in-phase moment coefficients over the range of $1/k$ greater than 1.5.

The experimental damping-moment-component coefficients and the theoretical damping-moment-component coefficients are shown in figure 7. The two-dimensional-flow theory is given again for reference only and, of course, needs large correction factors to make it apply to the data. The scatter in the data in conjunction with the possible influence of Mach number and of Reynolds number precludes exact conclusions with respect to the agreement of the data with the theoretical coefficients of the aspect-ratio theories. Although each of the aspect-ratio theories is to some extent in agreement with measured coefficients for the damping

moment over some range of $1/k$, it may be noted that neither aspect-ratio theory covers the overall range adequately.

The phase angle between the moment vector and the angular-position vector was obtained from the ratio of the out-of-phase and in-phase moment coefficients and is shown in figure 8. The scatter in the data is attributed to the scatter present in the components of the moment coefficients. It may be seen that the measured coefficients are in fair agreement with the coefficients given by the aspect-ratio theory of Reissner for $1/k$ greater than 2, whereas the theory of Lawrence and Gerber gives slightly lower values. In this instance, it appears that the two-dimensional-flow theory predicts substantially the same values as the aspect-ratio theories although it is slightly different in trend.

Before closing the discussion on the measured aerodynamic coefficients, it is appropriate to mention the possible influence of wind-tunnel-wall effects on the measured quantities. An analytical investigation (ref. 9) of the effects of wind-tunnel walls on air forces on a two-dimensional oscillating wing at subsonic speed demonstrated the possibility, under certain conditions, of the existence of large tunnel-wall effects, associated with an acoustic resonance phenomenon. It was also pointed out that similar conditions exist for three-dimensional flow. It was shown in this reference that a condition for a maximum of distortion is satisfied by the equation $M_{cr} = \sqrt{1 - \frac{\omega^2 H^2}{\pi^2 a^2}}$ where M_{cr} is the Mach number corresponding to the circular frequency of oscillation ω and tunnel height H at which the phenomenon will occur. The symbol a represents the speed of sound. At the present time, no quantitative calculations for a finite wing are available.

For the purpose of showing the proximity of the data reported herein to the region of critical tunnel-wall interference based on two-dimensional flow, plots of k against M for the various torsion springs are shown with a curve of critical tunnel-wall effects in figure 9. The curves marked A, B, C, and D are well away from the curve of critical wall effects and, thus, the tunnel-wall effects might be expected to be small. The range of critical Mach number M_{cr} for the data given in this paper is between 0.89 and 0.96, whereas the highest Mach number reported is 0.81. The curve marked D' intersects the critical curve at a value of $M = 0.47$ or $k = 0.77$ and represents data from spring D in Freon-12. Some evidence of the tunnel-wall effects based on the D' curve is shown in appendix C.

CONCLUDING REMARKS

Some measurements of the oscillating aerodynamic forces and moments acting on a rectangular wing of aspect ratio 2 oscillating about the midchord were made at four different frequencies. The measurements were made over a range of Mach number from 0.15 to 0.81, a range of Reynolds number from 0.60×10^6 to 9.21×10^6, and a range of reduced frequency from 0.15 to 1.32.

Appendixes are presented to show the correction of the root reaction for inertia and aeroelastic effects in order to determine the total aerodynamic load, to show the determination of the aerodynamic damping-moment coefficient, and to show some experimental evidence of wind-tunnel-wall effects on an oscillating wing.

A study of the effects of Mach number and Reynolds number indicated that, in the range of the experiment, the overall effects appeared to be small, although there were insufficient data even to determine qualitatively their trends. The phase angle between the lift vector and angular position was seen to vary fairly linearly over the range of reduced-frequency parameter studied. The in-phase lift and the in-phase moment remained essentially constant with change in frequency parameter, whereas the quadrature lift and quadrature moment were found to increase with an increase in frequency parameter.

Comparisons of the data were made with existing published data and with theoretical incompressible coefficients obtained from the aspect-ratio theory of Reissner, the aspect-ratio theory of Lawrence and Gerber, and the two-dimensional-flow theory. A comparison of the experimental data of this paper with other experimental data showed that good agreement was obtained for those coefficients that could be accurately determined. In the comparison of these data with the theoretical coefficients it was found, as might be expected, that the two-dimensional-flow theory was inadequate for predicting the experimental coefficients. However, the coefficients given by the aspect-ratio theories were generally in good agreement with the experimental data.

Langley Aeronautical Laboratory,
National Advisory Committee for Aeronautics,
Langley Field, Va., June 17, 1953.

APPENDIX A

CORRECTION OF ROOT REACTION FOR INERTIA AND AEROELASTIC EFFECTS TO DETERMINE THE TOTAL AERODYNAMIC LOAD

In the present experiment on a cantilever wing, knowledge is desired of the total aerodynamic load which develops solely from the torsional oscillations of the wing. This aerodynamic load is not equal precisely to the reaction at the wing root because of the presence of secondary bending reactions which come as a result of the freedom of the wing to be excited slightly in a bending oscillation. A correction must, therefore, be applied to the measured root reaction to obtain the aerodynamic load associated directly with the torsional motion. This appendix derives and shows the magnitude of this correction. The derivation is made in general terms of a wing of variable cross section; the correction is then applied to the uniform wing.

On the basis of the engineering beam theory, the differential equation for bending of the wing is

$$(1 + ig)\frac{\partial^2}{\partial x^2} EI \frac{\partial^2 y}{\partial x^2} = p \tag{A1}$$

where g is the structural damping coefficient and p is the intensity of the applied loading. When strip analysis approach is chosen, the loading for the case under consideration may be written

$$p = -m\ddot{y} - \frac{\pi\rho c^2}{4}\ddot{y} - \frac{a}{2}\rho cv(F + iG)\dot{y} + P \tag{A2}$$

The first term in this expression is the inertia force associated with the wing mass; the second and third terms refer, respectively, to the "apparent air-mass" inertia effect and the aerodynamic damping associated with bending oscillations; and the fourth term P refers to the torsionally induced aerodynamic loading, which here is regarded as the "applied forcing function." The second and third terms were established by using oscillating-flow theory for two-dimensional incompressible flow as a guide; the lift-curve slope a and the F and G coefficients, which are like the in-phase and out-of-phase Theodorsen flutter coefficients, are to be selected as appropriate to the case being treated.

Since harmonic motion is involved, the loading and the deflection may be written

$$P = L(x)e^{i\omega t} \tag{A3a}$$

$$y = Y(x)e^{i\omega t} \tag{A3b}$$

Now, with the use of equations (A2) and (A3), equation (A1) reduces to

$$(1 + ig)\frac{d^2}{dx^2} EI \frac{d^2Y}{dx^2} = \omega^2\bar{m}Y - i\frac{a}{2}\rho cv\omega(F + iG)Y + L \tag{A4}$$

where

$$\bar{m} = m + \frac{\pi\rho c^2}{4}$$

A convenient and fairly accurate approximate solution to this equation can be obtained by expressing the deflection in terms of the fundamental bending vibration mode of the wing, the choice here of only a single mode expansion being considered adequate since the forcing frequencies used in the experiments were below the fundamental wing frequency. Thus,

$$Y = a_1 y_1 \tag{A5}$$

where a_1 represents the response amplitude to be determined and y_1 is given in terms of unit tip amplitude and satisfies the equation

$$\frac{d^2}{dx^2} EI \frac{d^2y_1}{dx^2} = \omega_1^2\bar{m}y_1 \tag{A6}$$

In accordance with the Galerkin procedure for solving differential equations, equation (A5) is substituted into equation (A4) which is then multiplied by y_1 and integrated over the semispan of the wing. The result, with the use of equation (A6), is

$$a_1(1 + ig)\omega_1^2 M_1 = a_1\omega^2 M_1 - ia_1 \frac{a}{\pi} \frac{m_r}{k} \omega^2(F + iG)A_1 + \int_0^s Ly_1 \, dx \tag{A7}$$

where

$$M_1 = \int_0^s \bar{m} y_1^2 dx$$

$$A_1 = \int_0^s \frac{c}{c_r} y_1^2 dx$$

$$m_r = \frac{\pi \rho c_r^2}{4}$$

$$k = \frac{\omega c_r}{2v}$$

and c_r is some convenient reference chord, usually taken at about the three-quarter-span station. The desired response amplitude can now be determined directly from equation (A7); hence,

$$a_1 = \frac{\int_0^s Ly_1 \, dx}{(\omega_1^2 - \omega^2)M_1 - \frac{a}{\pi} \frac{G}{k} m_r A_1 \omega^2 + i\left(g\omega_1^2 M_1 + \frac{a}{\pi} \frac{F}{k} m_r A_1 \omega^2\right)} \tag{A8}$$

The loading on the beam is now written in terms of a_1. Substitution of equations (A3) and (A5) into equation (A2) gives

$$p = \left\{\left[m\omega_1^2 y_1 + \frac{\pi \rho c^2}{4} \omega^2 y_1 - i \frac{a}{2} \rho c v \omega (F + iG) y_1\right] a_1 + L\right\} e^{i\omega t}$$

The root shear or reaction, which may be designated $V_o e^{i\omega t}$, may be found by integrating this loading over the length of the beam; thus,

$$V_o e^{i\omega t} = \left\{ \left[\omega^2 N_1 - i(F + iG) \frac{a}{\pi} \frac{m_r \omega^2}{k} B_1 \right] a_1 + \int_0^s L \, dx \right\} e^{i\omega t} \tag{A9}$$

where

$$N_1 = \int_0^s \bar{m} y_1 \, dx$$

$$B_1 = \int_0^s \frac{c}{c_r} y_1 \, dx$$

Substitution of equation (A8) into equation (A9) and cancellation of the harmonic terms gives

$$V_o = \left[1 + \frac{(C_1 + iC_2)d}{D_1 + iD_2} \right] \int_0^s L \, dx \tag{A10}$$

where

$$\left.\begin{aligned} C_1 &= \frac{N_1}{M_1} + \frac{a}{\pi} \frac{G}{k} \frac{m_r B_1}{M_1} \\ C_2 &= - \frac{a}{\pi} \frac{F}{k} \frac{m_r B_1}{M_1} \\ D_1 &= \frac{\omega_1^2}{\omega^2} - 1 - \frac{a}{\pi} \frac{G}{k} \frac{m_r A_1}{M_1} \\ D_2 &= g \frac{\omega_1^2}{\omega^2} + \frac{a}{\pi} \frac{F}{k} \frac{m_r A_1}{M_1} \\ d &= \frac{\int_0^s L y_1 \, dx}{\int_0^s L \, dx} \end{aligned}\right\} \tag{A11}$$

As stated earlier, knowledge is desired of the total aerodynamic load that is associated with the torsional oscillations of the wing. This total load is found directly from equation (A10) to be

$$\int_0^s L\,dx = \frac{D_1 + iD_2}{C_1 d + D_1 + i(C_2 d + D_2)} V_o$$

This equation, when expressed in the complex notation of a modulus and a phase angle, becomes

$$\int_0^s L\,dx = \sqrt{\frac{D_1^2 + D_2^2}{(C_1 d + D_1)^2 + (C_2 d + D_2)^2}}\, e^{i\phi_1 \frac{\pi}{180}} V_o = K e^{i\phi_1 \frac{\pi}{180}} V_o \quad (A12)$$

where

$$\phi_1 \frac{\pi}{180} = \tan^{-1} \frac{(C_1 D_2 - C_2 D_1) d}{d(C_1 D_1 + C_2 D_2) + D_1^2 + D_2^2} \quad (A13)$$

This is the final equation sought. Thus, the magnitude of the torsionally induced air load is found simply by multiplying K by the magnitude of the measured root shear; the phase angle in radians between this load and the root shear is given by ϕ_1. A word about the coefficients C_n, D_n, and d may now be in order. All terms in these coefficients which contain the lift-curve slope a are related to the aerodynamic damping effects associated with the bending oscillations. A comparison of the second term with the first term in D_2, for example, will indicate how strong the aerodynamic damping is in relation to the structural damping. The nondimensional term d may be seen to depend on the distribution of the air load $L(x)$. For most practical cases, it is considered sufficient to evaluate this factor on the basis that the air load has an elliptic distribution.

Some simplification results when the aforementioned relations are applied to the case treated herein, that is, to a uniform cantilever wing. In this case, it is easily shown that

$$\left.\begin{aligned} M_1 &= \bar{m}\int_0^s y_1^2\,dx = \frac{\bar{m}s}{4} \\ N_1 &= \bar{m}\int_0^s y_1\,dx = 0.3915\bar{m}s \\ A_1 &= \int_0^s y_1^2\,dx = \frac{s}{4} \\ B_1 &= \int y_1\,dx = 0.3915s \end{aligned}\right\} \tag{A14}$$

Hence,

$$\left.\begin{aligned} C_1 &= 1.566\left(1 + \frac{a}{\pi}\frac{G}{k}\frac{m_r}{\bar{m}}\right) \\ C_2 &= -1.566\,\frac{a}{\pi}\frac{F}{k}\frac{m_r}{\bar{m}} \\ D_1 &= \frac{\omega_1^2}{\omega^2} - 1 - \frac{a}{\pi}\frac{G}{k}\frac{m_r}{\bar{m}} \\ D_2 &= g\,\frac{\omega_1^2}{\omega^2} + \frac{a}{\pi}\frac{F}{k}\frac{m_r}{\bar{m}} \end{aligned}\right\} \tag{A15a}$$

and, for an assumed elliptic loading,

$$d = 0.29 \tag{A15b}$$

In order to determine the correction K and the phase angle ϕ_1 for the four different spring combinations that were used in the tests,

equations (A12) and (A13) were used together with equations (A15). The structural damping coefficient used for the wing was $g = 0.008$. The lift-curve slope was taken equal to the theoretical value of 2π multiplied by the often used aspect-ratio correction $\frac{A}{A + 2}$ and was thus taken as π since the wing is of aspect ratio 2. The F and G functions were arbitrarily chosen as those for two-dimensional incompressible flow. The results obtained for the four cases are shown in the following table:

Torsion spring	$\omega \times (2\pi)^{-1}$	Structural damping only, a = 0		Both structural and aerodynamic damping	
		K	ϕ_1, deg	K	ϕ_1, deg
A	31	0.98	0.012	0.98	0.06
B	43	.95	.030	.95	.11
C	54	.91	.060	.91	.19
D	62	.87	.093	.87	.30

In order to gain an insight as to how aerodynamic damping effects compare with structural damping effects, the calculations were made for two conditions: (1) with structural damping only and (2) with both structural and aerodynamic damping included. The table shows the results for these two conditions. No differences are noted in K for these two conditions. However, K decreases from a value of 0.98 to a value of 0.87 as the forcing frequency increases; thereby a correction that ranges from 2 to 13 percent is indicated. Although a difference in phase angle is noted for the two damping conditions, the important thing to note is that in all cases the phase angle is a negligible quantity.

APPENDIX B

DETERMINATION OF THE AERODYNAMIC DAMPING-MOMENT COEFFICIENT

In this appendix the method used in obtaining the aerodynamic damping-moment coefficient from the power-off decaying oscillations of a torsional spring-inertia system is given. By assuming a linear problem, particularly with respect to the aerodynamic coefficients, and by using the concept that the structural damping moment is in phase with the angular velocity but proportional to the angular displacement, the differential equation of motion of the system is given by

$$I_s\ddot{\alpha} + k_s\left(1 + ig_s\right)\alpha = \frac{\pi}{2}\rho v^2 s c^2 \alpha\left(m_1 + im_2\right) \tag{B1}$$

or

$$\ddot{\alpha} + \frac{C + iB}{A}\alpha = 0$$

where A, B, and C denote coefficients. By definition,

$$\frac{C}{A} = \frac{k_s - \frac{\pi}{2}\rho v^2 s c^2 m_1}{I_s} = \omega_1{}^2$$

and

$$\frac{B}{C} = \frac{k_s g_s - \frac{\pi}{2}\rho v^2 c^2 s m_2}{k_s - \frac{\pi}{2}\rho v^2 c^2 s m_1} = \lambda$$

Equation (B1) has a solution of the following form (see, for instance, page 86 of ref. 10):

$$\alpha = |\alpha| e^{\sqrt{\frac{C}{2A}}\left[-\sqrt{\left(1+\lambda^2\right)^{1/2}-1}+i\sqrt{\left(1+\lambda^2\right)^{1/2}+1}\right]t} \tag{B2}$$

For small values of λ, equation (B2) becomes

$$\alpha = |\alpha| e^{\omega_1 t\left[-\frac{\lambda}{2}+i\left(1+\frac{\lambda^2}{4}\right)\right]} \approx |\alpha| e^{\omega_1 t\left(-\frac{\lambda}{2}+i\right)} \tag{B3}$$

For the logarithmic decrement, equation (B3) at $t = 0$ becomes

$$|\alpha|_0 = |\alpha|$$

and, after n cycles, at $t = 2\pi n/\omega_1$,

$$|\alpha|_n = |\alpha| e^{-\pi\lambda n}$$

or

$$\frac{|\alpha|_0}{|\alpha|_n} = e^{\pi\lambda n} \tag{B4}$$

By taking the natural logarithm of both sides of equation (B4),

$$\lambda = \frac{1}{\pi n} \log_e \frac{|\alpha|_0}{|\alpha|_n} = g_t$$

which is measured with the wing subjected to air flow. From the definition of λ,

$$g_t = \frac{k_s g_s - \frac{\pi}{2}\rho v^2 c^2 s m_2}{k_s - \frac{\pi}{2}\rho v^2 c^2 s m_1} \tag{B5}$$

Since

$$k_s - \frac{\pi}{2} \rho v^2 c^2 s m_1 = I_s \omega_1^2$$

and

$$k_s = I_s \omega_{vac}^2$$

then

$$-m_2 = \frac{I_s \omega_1^2}{\frac{\pi}{2} \rho v^2 c^2 s} \left[g_t - \left(\frac{\omega_{vac}}{\omega_1} \right)^2 g_s \right] \tag{B6}$$

Equation (B6) is the form used in the reduction of the damping-moment data in this paper.

APPENDIX C

SOME EXPERIMENTAL EVIDENCE OF WIND-TUNNEL-WALL EFFECTS ON AN OSCILLATING WING

This appendix is presented to document data relating to some wind-tunnel-wall effects on oscillating air forces and moments. The problem of the effect of the presence of wind-tunnel walls on measurements pertaining to airfoils and wings in the steady-state case has been resolved. The problem for the condition of unsteady flow has been treated theoretically by Reissner in reference 11, Jones in reference 12, and Timman in reference 13 for the incompressible case, and by Runyan and Watkins in reference 9 for the two-dimensional subsonic compressible case. For the incompressible-flow condition, the influence of the tunnel walls has been found to be comparatively small for most cases, although indications are given that, for some ranges of $2v/c\omega$, the effect may be very large. For the compressible-flow case, reference 14 indicates the possibility of obtaining a resonant condition which might result in a misinterpretation of the measured quantities, the critical condition for the rectangular tunnel being given by $\omega H/a = (2m - 1)\pi\sqrt{1 - M^2}$ where $m = 1$, 2, and 3.

Reference 9 indicates that this resonant condition corresponds to the establishment of transverse velocities having a maximum amplitude at the airfoil. These transverse velocity components alter the effective angle of attack and thus affect the air forces. Such a condition might be expected to be obtained for the finite wing, although the behavior of the measured forces and moments in approaching the vicinity of the "critical" condition may not necessarily follow the pattern of the two-dimensional wing.

An indication that a distortion and a resonance is experienced by oscillating wings has been obtained experimentally. These data are presented in table VIII and figures 10 and 11. It might be remarked that the phenomena have also been observed for the two-dimensional wing in connection with the work of reference 5. The peculiar behavior of the data in the neighborhood of the Mach number which is critical for the resonance condition is strikingly demonstrated by the damping-moment coefficients. (See fig. 10.) For the finite wing, these data tend to yield peak values of the damping-moment coefficients in the vicinity of the "critical Mach number." It is of interest to note that this behavior is the inverse to that observed for the data of the infinite wing of reference 13. This inversion may be attributed to the introduction of three-dimensional effects into the problem.

Figure 11 indicates effects of wall interference on the oscillating lift coefficients. As the critical value of $1/k$ is reached, the lift coefficient drops off and there is a definite dip in the curve.

These data have been presented to furnish some evidence of the nature of the effects of tunnel walls on the aerodynamic forces and moments acting on an oscillating wing. It is evident that some caution is required to avoid conditions leading to these effects.

REFERENCES

1. Williams, J.: Aircraft Flutter. R. & M. No. 2492, British A.R.C., 1948.

2(a). Reissner, Eric: Effect of Finite Span on the Airload Distributions for Oscillating Wings. I - Aerodynamic Theory of Oscillating Wings of Finite Span. NACA TN 1194, 1947.

(b). Reissner, Eric, and Stevens, John E.: Effect of Finite Span on the Airload Distributions for Oscillating Wings. II - Methods of Calculation and Examples of Application. NACA TN 1195, 1947.

3. Lawrence, H. R., and Gerber, E. H.: The Aerodynamic Forces on Low Aspect Ratio Wings Oscillating in an Incompressible Flow. Jour. Aero. Sci., vol. 19, no. 11, Nov. 1952, pp. 769-781. (Errata issued, vol. 20, no. 4, Apr. 1953, p. 296.) (Also available as Rep. No. AF-781-A-1, Cornell Aero. Lab., Inc., Jan. 1952.)

4. Theodorsen, Theodore: General Theory of Aerodynamic Instability and the Mechanism of Flutter. NACA Rep. 496, 1935.

5. Clevenson, Sherman A., and Widmayer, Edward Jr.: Experimental Measurements of Forces and Moments of a Two-Dimensional Oscillating Wing at Subsonic Speeds. NACA TN 3686, 1956. (Supersedes NACA RM L9K28a.)

6. Ashley, H., Zartarian, G., and Neilson, D. O.: Investigation of Certain Unsteady Aerodynamic Effects in Longitudinal Dynamic Stability. USAF Tech. Rep. No. 5986 (Contract No. AF 33(038)-11668, RDO No. R458-414b), Wright Air Dev. Center, U. S. Air Force, M.I.T., Dec. 1951.

7. Bratt, J. B., and Wight, K. C.: The Effect of Mean Incidence, Amplitude of Oscillation, Profile, and Aspect Ratio on Pitching Moment Derivatives. R. & M. No. 2064, British A.R.C., 1945.

8. Houbolt, John C.: A Recurrence Matrix Solution for the Dynamic Response of Aircraft in Gusts. NACA Rep. 1010, 1951. (Supersedes NACA TN 2060.)

9. Runyan, Harry L., and Watkins, Charles E.: Considerations on the Effect of Wind-Tunnel Walls on Oscillating Air Forces for Two-Dimensional Subsonic Compressible Flow. NACA Rep. 1150, 1953. (Supersedes NACA TN 2552.)

10. Scanlan, Robert H., and Rosenbaum, Robert: Introduction to the Study of Aircraft Vibrations and Flutter. The Macmillan Co., 1951.

11. Reissner, E.: Wind Tunnel Corrections for the Two-Dimensional Theory of Oscillating Airfoils. Rep. No. SB-218-S-3, Cornell Aero. Lab., Inc., Apr. 22, 1947.

12. Jones, W. Prichard: Wind Tunnel Interference Effect on the Values of Experimentally Determined Derivative Coefficients for Oscillating Aerofoils. R. & M. No. 1912, British A.R.C., Aug. 1943.

13. Timman, R.: The Aerodynamic Forces on an Oscillating Aerofoil Between Two Parallel Walls. Appl. Sci. Res. (The Hague), vol. A 3, no. 1, 1951, pp. 31-57.

14. Runyan, Harry L., Woolston, Donald S., and Rainey, A. Gerald: Theoretical and Experimental Investigation of the Effect of Tunnel Walls on the Forces on an Oscillating Airfoil in Two-Dimensional Subsonic Compressible Flow. NACA Rep 1262, 1956. (Supersedes NACA TN 3416.)

TABLE I.- EXPERIMENTAL DATA FOR TORSIONAL SPRING A

[Test Medium: Air and Freon-12 Mixture]

ρ	v	M	k	$1/k$	$\lvert\alpha\rvert$	R	ϕ	$\frac{\lvert L\rvert}{\pi\rho v^2 sc\lvert\alpha\rvert}$	l_1	l_2	θ	m_1	m_2	$\frac{\lvert M_\alpha\rvert}{2\left(\frac{\pi}{2}\right)\rho v^2 sc^2\lvert\alpha\rvert}$
$8,486 \times 10^{-6}$	112.80	0.224	0.8627	1.16	0.03087	3.59×10^6	42.7	1.279	0.940	0.867	-15	0.7068	-0.1879	0.732
8,333	156.00	.312	.6142	1.63	.03045	4.92	32.9	1.108	.950	.602	-19	.4595	-.1524	.484
8,209	187.70	.375	.5038	1.99	.03073	5.84	27.4	1.023	.908	.471	-19	.4479	-.1500	.472
8,064	211.22	.422	.4418	2.26	.03003	6.43	21.3	1.008	.939	.366	-17	.4602	-.1395	.482
7,879	243.29	.486	.3784	2.64	.02857	7.23	21.7	1.138	1.057	.421	-22	.4310	-.1700	.463
7,625	282.54	.563	.3220	3.10	.02990	8.11	17.3	.924	.882	.275	-18	.3736	-.1222	.393
7,445	309.14	.615	.2866	3.49	.02990	8.65	14.8	.911	.880	.233	-17	.4171	-.1252	.437
7,227	340.37	.674	.2548	3.93	.02976	9.21	15.2	.875	.845	.229	-18	.4135	-.1377	.436
5,779	132.28	.260	.7267	1.38	.03183	2.85	41.0	1.040	.785	.682	-11	.8330	-.1666	.849
5,692	160.12	.315	.6024	1.66	.03073	3.40	35.8	.996	.808	.583	-17	.5135	-.1499	.535
5,571	198.64	.392	.4792	2.09	.03114	4.14	28.2	.970	.855	.458	-16	.5072	-.1455	.528
5,479	224.35	.443	.4187	2.39	.03100	4.60	25.7	.979	.882	.424	-15	.5366	-.1379	.554
5,358	251.88	.497	.3692	2.71	.03045	5.05	20.2	.978	.918	.338	-16	.5136	-.1432	.534
5,240	277.84	.548	.3347	2.99	.02976	5.43	20.1	.975	.915	.335	-19	.4317	-.1501	.457
5,024	322.50	.636	.2825	3.54	.02976	6.05	12.6	.989	.965	.216	-20	.4362	-.1528	.462
4,932	340.95	.670	.2645	3.78	.02976	6.26	12.9	1.042	1.016	.233	-20	.4434	-.1620	.472
4,852	353.28	.703	.2455	4.07	.02828	6.44	9.4	1.102	1.087	.180	-20	.5058	-.1810	.535

NACA

TABLE II.- EXPERIMENTAL DATA FOR TORSIONAL SPRING B

[Test Medium: Air]

ρ	v	M	k	l/k	$\lvert\alpha\rvert$	R	ϕ	$\frac{\lvert L\rvert}{\pi\rho v^2 sc\lvert\alpha\rvert}$	l_1	l_2	θ	m_1	m_2	$\frac{\lvert M_\alpha\rvert}{\frac{1}{2}\rho v^2 sc^2\lvert\alpha\rvert}$
$2{,}369 \times 10^{-6}$	286.92	0.261	0.4510	2.218	0.02391	1.872×10^6	28.1	0.929	0.820	0.438	-12	0.6043	-0.1313	0.618
2,312	353.07	.320	.3673	2.72	.02448	2.241	20.9	.918	.857	.327	-17	.3706	-.1129	.387
2,135	409.32	.360	.3161	3.16	.02433	2.306	16.7	.938	.898	.270	-16	.3293	-.0934	.342
2,256	410.44	.371	.3116	3.21	.02433	2.533	16.5	.942	.904	.268	-13	.4489	-.1061	.461
2,206	460.26	.415	.2779	3.60	.02391	2.769	12.5	.986	.962	.213	-16	.3651	-.1035	.379
2,168	488.51	.440	.2592	3.85	.02376	2.880	13.8	.925	.899	.221	-13	.4103	-.0950	.421
2,140	510.64	.459	.2479	4.03	.02419	2.958	16.1	.941	.904	.261	-14	.3807	-.0924	.392
2,103	539.47	.485	.2330	4.29	.02348	3.058	13.7	.956	.929	.227	-12	.3968	-.0804	.405
2,066	563.81	.505	.2235	4.47	.02391	3.130	7.3	.995	.987	.126	-14	.3546	-.0892	.366
2,019	598.00	.533	.2090	4.79	.02391	3.250	13.3	.954	.929	.219	-16	.3647	-.1025	.379
1,965	640.14	.568	.1914	5.22	.02334	3.346	6.2	.964	.958	.104	-12	.4672	-.0981	.477
1,094	334.71	.301	.3905	2.56	.02362	.9926	23.6	.964	.883	.386	-11	.6131	-.1223	.625
1,081	371.14	.319	.3554	2.81	.02533	1.0243	22.0	.897	.832	.336	-22	.2317	-.0883	.248
1,069	428.34	.385	.3051	3.28	.02419	1.2429	14.2	.903	.876	.222	-16	.3832	-.1069	.398
1,050	482.05	.434	.2699	3.71	.02448	1.3732	15.2	.938	.906	.246	-14	.3966	-.0982	.409
1,033	535.54	.482	.2411	4.15	.02391	1.5004	13.1	.885	.862	.201	-12	.4357	-.0895	.445
1,010	598.46	.538	.2152	4.87	.02448	1.6372	9.1	.944	.932	.149	-13	.3842	-.0867	.394
982	666.25	.597	.1909	5.24	.02419	1.7649	11.3	.965	.947	.189	-13	.4395	-.0970	.450
954	729.72	.653	.1735	5.76	.02405	1.8744	12.5	.931	.909	.202	-13	.4176	-.0945	.428
940	775.98	.692	.1631	6.13	.02433	1.9571	8.0	.967	.957	.135	-14	.3751	-.0933	.387
905	848.14	.754	.1463	6.84	.02362	2.0507	6.2	1.047	1.041	.113	-10	.4518	-.0945	.462
566	463.41	.410	.2820	3.55	.02476	.6967	14.8	.868	.839	.222	-9	.6184	-.1048	.627
553	549.49	.488	.2389	4.19	.02504	.8112	13.3	.85	.827	.196	-15	.3234	-.0828	.333
537	637.87	.568	.2040	4.90	.02533	.9161	10.4	.847	.835	.153	-11	.4429	-.0848	.451
520	716.55	.638	.1806	5.54	.02490	.9963	11.3	.941	.923	.184	-13	.4417	-.0979	.452
501	797.44	.710	.1619	6.18	.02462	1.0699	7.4	.987	.979	.127	-15	.4038	-.1067	.418
480	880.99	.784	.1447	6.92	.02533	1.1316	3.4	.995	.994	.059	-12	.4862	-.0995	.496

TABLE III.- EXPERIMENTAL DATA FOR TORSIONAL SPRING C

Test Medium: Air

ρ	v	M	k	1/k	$\lvert\alpha\rvert$	R	ϕ	$\frac{\lvert I\rvert}{\pi\rho v^2 sc\lvert\alpha\rvert}$	l_1	l_2	m_2
$2{,}328 \times 10^{-6}$	204.51	0.183	0.8185	1.222	0.02351	0.6035×10^6	39.3	1.040	0.805	0.659	-0.1582
2,305	246.29	.220	.6773	1.475	.02305	1.040	31.9	.989	.840	.523	-.1351
2,275	295.72	.264	.5630	1.775	.02318	1.231	33.4	.997	.832	.549	-.1226
2,243	332.67	.297	.4996	2.000	.02318	1.36	29.7	.880	.764	.436	-.1169
2,219	364.48	.325	.4568	2.19	.02351	1.477	29.4	.945	.839	.435	-.1137
2,188	397.35	.353	.4087	2.45	.02305	1.537	26.4	1.026	.919	.456	-.1104
2,132	445.76	.395	.3673	2.72	.02318	1.718	22.8	.978	.902	.379	-.1042
2,086	491.22	.435	.3306	3.03	.02357	1.858	17.0	1.006	.962	.294	-.1092
2,024	550.94	.487	.2948	3.395	.02318	2.015	20.8	1.006	.940	.357	-.1089
1,973	595.01	.525	.2692	3.71	.02252	2.091	17.0	.907	.867	.265	-.1180
1,919	641.18	.562	.2499	4.00	.02239	2.204	14.3	.857	.850	.212	-.1146
1,370	301.39	.258	.5441	1.838	.02409	1.031	29.5	.832	.724	.409	-.1175
1,332	424.59	.363	.3863	2.59	.02351	1.414	23.8	.877	.802	.354	-.1059
1,247	625.72	.537	.2621	3.82	.02351	1.975	15.6	.966	.930	.260	-.0994
1,128	326.69	.280	.5069	1.972	.02396	.925	33.3	.861	.720	.473	-.1091
1,108	392.43	.336	.4243	2.355	.02396	1.089	27.2	.863	.768	.395	-.1025
1,078	476.54	.407	.3448	2.90	.02344	1.284	28.2	.904	.797	.427	-.0948
1,055	546.62	.468	.3000	3.333	.02385	1.449	21.2	.928	.865	.335	-.0977
1,044	589.65	.506	.2771	3.61	.02357	1.552	15.8	.969	.932	.264	-.0983
1,022	633.10	.543	.2595	3.85	.02305	1.627	15.4	.922	.889	.245	-.1024
996	689.68	.592	.2355	4.25	.02409	1.738	19.0	.934	.883	.304	-.1028
962	776.25	.672	.2084	4.80	.02239	1.930	8.9	1.028	1.015	.159	-.1138
966	800.29	.691	.2002	5.00	.02292	1.995	12.0	1.001	.979	.208	-.1351
946	815.95	.712	.1971	5.08	.02239	2.018	1.8	1.031	1.031	.032	-.1299
908	878.41	.775	.1824	5.48	.02174	2.113	9.6	.914	.901	.152	-.1656
629	525.76	.462	.3161	3.16	.02331	.871	18.9	.780	.738	.253	-.0988
610	603.93	.532	.2742	3.65	.02265	.975	11.2	.933	.915	.181	-.0923
594	672.97	.595	.2450	4.08	.02265	1.061	10.7	.976	.959	.181	-.1035
572	752.85	.669	.2208	4.53	.02265	1.150	16.4	1.021	.980	.288	-.1180
569	784.31	.689	.2087	4.79	.02318	1.176	14.3	.976	.945	.241	-.1297
567	812.53	.714	.2015	4.97	.02292	1.216	9.4	1.016	1.002	.166	-.1237
550	823.47	.736	.1992	5.02	.02305	1.217	6.9	1.056	1.049	.127	-.1267
551	846.45	.750	.1934	5.18	.02226	1.240	9.8	1.118	1.102	.190	-.1458
525	900.51	.812	.1825	5.47	.02161	1.283	13.4	1.278	1.244	.296	-.1455

NACA

TABLE IV.- EXPERIMENTAL DATA FOR TORSIONAL SPRING D

[Test Medium: Air]

ρ	v	M	k	1/k	$\lvert\alpha\rvert$	R	ϕ	$\frac{\lvert L\rvert}{\pi\rho v^2 sc\lvert\alpha\rvert}$	l_1	l_2	m_2
$2{,}083 \times 10^{-6}$	174.91	0.148	1.0902	0.916	0.03680	0.893×10^6	31.76	1.565	1.330	0.824	-0.3812
2,076	214.54	.181	.8962	1.115	.03653	1.093	34.59	1.230	1.012	.698	-.2886
2,056	243.67	.206	.7890	1.268	.03598	1.229	27.57	1.299	1.151	.601	-.2336
2,045	273.50	.231	.6915	1.448	.03598	1.374	26.90	1.247	1.112	.564	-.2162
2,032	298.71	.253	.6384	1.565	.03516	1.491	27.95	1.158	1.023	.543	-.1902
2,021	323.63	.274	.5883	1.700	.03434	1.611	30.44	1.033	.891	.523	-.1824
2,027	352.96	.301	.5358	1.870	.03078	1.780	30.24	.905	.782	.456	-.1402
2,018	370.90	.316	.5099	1.960	.03256	1.864	27.09	.860	.766	.392	-.1472
2,000	396.14	.338	.4814	2.08	.03283	1.976	24.77	.894	.811	.374	-.1350
1,990	413.83	.353	.4547	2.20	.03160	2.055	28.21	.921	.811	.435	-.1350
1,967	435.42	.371	.4322	2.31	.03201	2.132	23.19	.844	.776	.332	-.1250
1,938	457.08	.389	.4131	2.42	.03119	2.199	20.75	.943	.882	.334	-.1234
1,966	493.41	.421	.3788	2.64	.02900	2.422	13.70	.844	.821	.1999	-.1162
1,949	518.47	.442	.3623	2.76	.02763	2.516	12.52	.920	.898	.199	-.1072
1,946	533.26	.455	.3458	2.89	.02627	2.588	12.29	.894	.873	.190	-.1134
1,940	548.96	.468	.3365	2.97	.02654	2.653	12.31	.929	.907	.198	-.1212
1,868	557.42	.470	.3353	2.98	.03694	2.55	13.39	.726	.707	.168	-.1192
1,867	572.09	.484	.3284	3.05	.02845	2.63	13.45	.937	.911	.218	-.1082
1,998	577.12	.492	.3244	3.08	.02627	2.871	11.23	.897	.880	.175	-.1092
1,871	588.00	.500	.3174	3.16	.02804	2.73	8.90	.982	.971	.152	-.1190
1,871	605.92	.517	.3075	3.25	.02668	2.83	8.88	1.053	1.040	.163	-.1146
1,902	608.13	.518	.3063	3.26	.02462	2.877	9.93	1.018	1.003	.175	-.1172
1,870	624.44	.536	.3004	3.33	.02620	2.94	8.94	.995	.983	.155	-.1216
1,868	642.64	.554	.2918	3.43	.02544	3.04	8.94	1.060	1.048	.165	-.1384

TABLE V.- THEORETICAL INCOMPRESSIBLE COEFFICIENTS OF REISSNER APPLIED AT ASPECT RATIO 2

k	1/k	ϕ	$\frac{\lvert L\rvert}{\pi\rho v^2 sc\lvert\alpha\rvert}$	l_1	l_2	θ	m_1	m_2
0.15	6.67	8.08	0.9412	0.9320	0.1315	-10.25	0.4684	-0.0848
.20	5.00	11.01	.9519	.9344	.1819	-9.15	.4704	-.0759
.25	4.00	14.50	.9550	.9244	.2396	-15.28	.4736	-.1296
.40	2.50	24.20	1.0106	.9288	.3984	-21.80	.5044	-.2020
.60	1.67	33.90	1.1480	.9530	.6400	-26.00	.5644	-.2752
.80	1.25	44.70	1.3050	.9272	.9184	-28.70	.6232	-.3412
1.00	1.00	52.50	1.5706	.9564	1.2456	-27.30	.7292	-.3768

NACA

TABLE VI.- THEORETICAL INCOMPRESSIBLE COEFFICIENTS OF LAWRENCE AND GERBER FOR ASPECT RATIO 2

k	1/k	ϕ	$\frac{\lvert L\rvert}{\pi\rho v^2 sc\lvert\alpha\rvert}$	l_1	l_2	θ	$\frac{M_\alpha}{\frac{\pi}{2}\rho v^2 sc^2\lvert\alpha\rvert}$	m_1	m_2
0.125	8.0	8.9	0.787	0.777	0.121	-5.0	0.455	0.453	-0.0394
.25	4.0	18.2	.802	.764	.250	-9.3	.457	.452	-.0737
.5	2.0	35.3	.910	.743	.526	-15.9	.478	.560	-.131
1.0	1.0	54.6	1.1233	.718	1.10	-24.1	.583	.532	-.238

NACA

TABLE VII.- TWO-DIMENSIONAL INCOMPRESSIBLE COEFFICIENTS OF THEODORSEN

k	1/k	ϕ	$\frac{\lvert L \rvert}{\pi\rho v^2 sc \lvert\alpha\rvert}$	l_1	l_2	θ	m_1	m_2
0.20	5.00	-1.21	1.493	1.490	-0.0317	-16.0	0.752	-0.2158
.30	3.33	5.82	1.390	1.384	.141	-18.0	.703	-.2258
.40	2.50	13.66	1.354	1.316	.320	-19.5	.678	-.2400
.50	2.00	21.35	1.365	1.271	.497	-20.7	.667	-.2512
.60	1.67	28.40	1.410	1.240	.672	-21.8	.665	-.2641
.80	1.25	40.05	1.570	1.201	1.010	-23.4	.681	-.2948
1.00	1.00	48.60	1.784	1.179	1.339	-24.9	.715	-.3306
1.20	.83	54.95	2.029	1.165	1.661	-25.9	.763	-.3697

TABLE VIII.- EXPERIMENTAL DATA SHOWING EFFECT OF WIND-TUNNEL-WALL INTERFERENCE FOR TORSIONAL SPRING D' IN FREON

ρ	v	M	k	1/k	$\lvert\alpha\rvert$	R	$\frac{\lvert L\rvert}{\pi\rho v^2 sc\lvert\alpha\rvert}$	m_2
$6{,}153 \times 10^{-6}$	358	0.668	0.514	1.94	0.01833	7.65×10^6	0.944	-0.251
6,194	351	.654	.527	1.90	.01956	7.55	.932	-.174
6,275	335	.624	.552	1.81	.02230	7.30	.813	-.104
6,350	323	.601	.584	1.71	.02175	7.10	.749	-.094
6,456	304	.566	.621	1.61	.01915	6.81	.782	-.244
6,507	296	.552	.630	1.59	.01847	6.69	.914	-.359
6,536	292	.543	.649	1.54	.01751	6.63	1.013	-.436
6,581	282	.524	.664	1.51	.01751	6.44	1.152	-.483
6,644	270	.503	.694	1.44	.01943	6.23	1.354	-.408
6,695	262	.487	.712	1.40	.02020	6.09	1.284	-.379
6,728	254	.472	.731	1.37	.02120	5.93	1.350	-.291
6,810	239	.443	.774	1.29	.02257	5.65	1.182	-.272
6,839	231	.429	.818	1.22	.02408	5.49	1.347	-.272
6,885	221	.410	.856	1.17	.02503	5.28	1.429	-.283
6,927	212	.395	.879	1.14	.02544	5.10	1.407	-.262
6,963	203	.378	.934	1.07	.02654	4.91	1.446	-.279
7,005	192	.357	.996	1.00	.02688	4.67	1.458	-.260
7,071	176	.327	1.065	.94	.02750	4.32	1.579	-.276
7,124	160	.298	1.172	.85	.02900	3.96	1.693	-.283
7,186	143	.267	1.317	.76	.02900	3.57	1.893	-.292

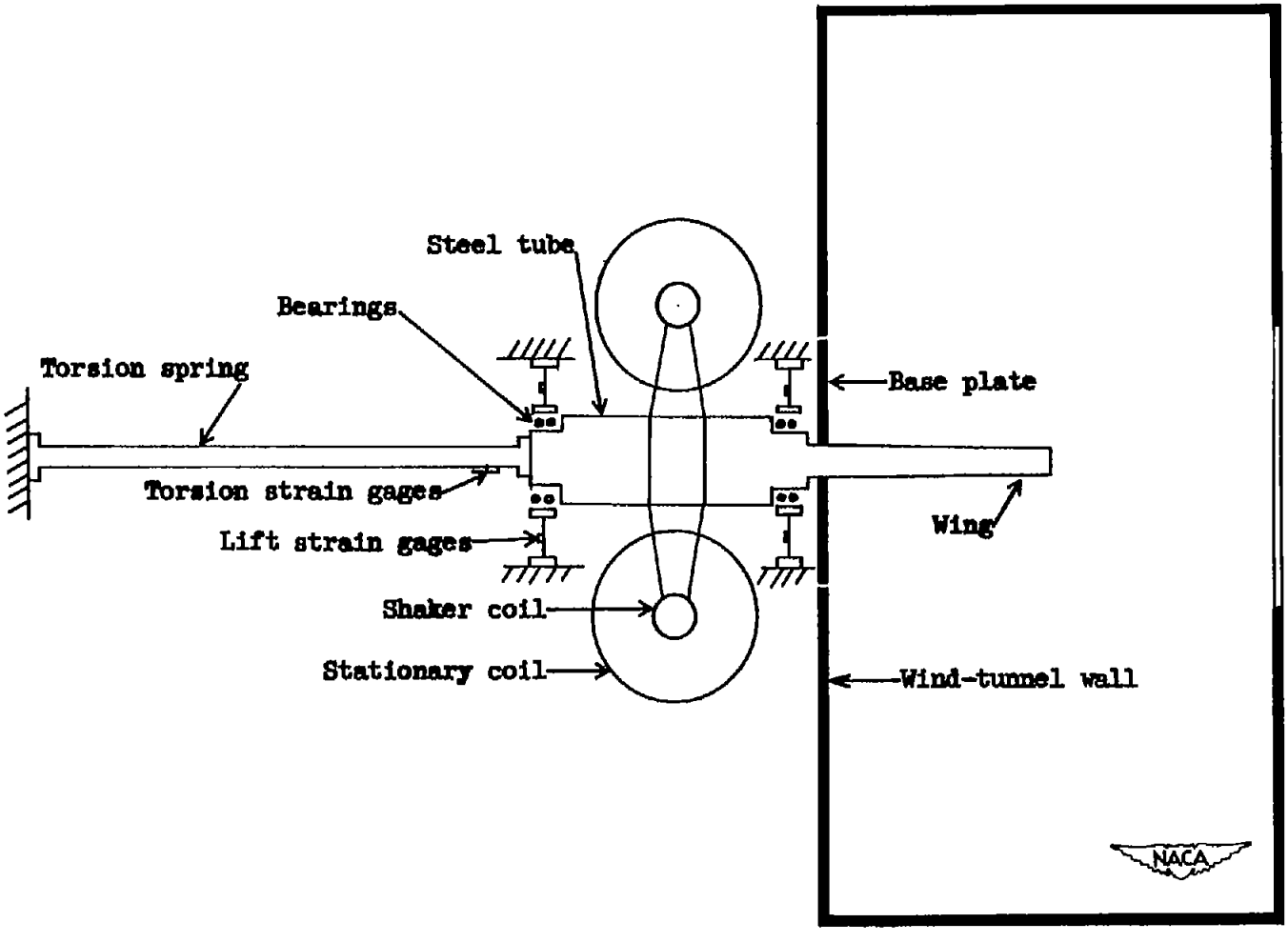

Figure 1.- Diagram of oscillating mechanism and wing mounted in the Langley 2- by 4-foot flutter research tunnel.

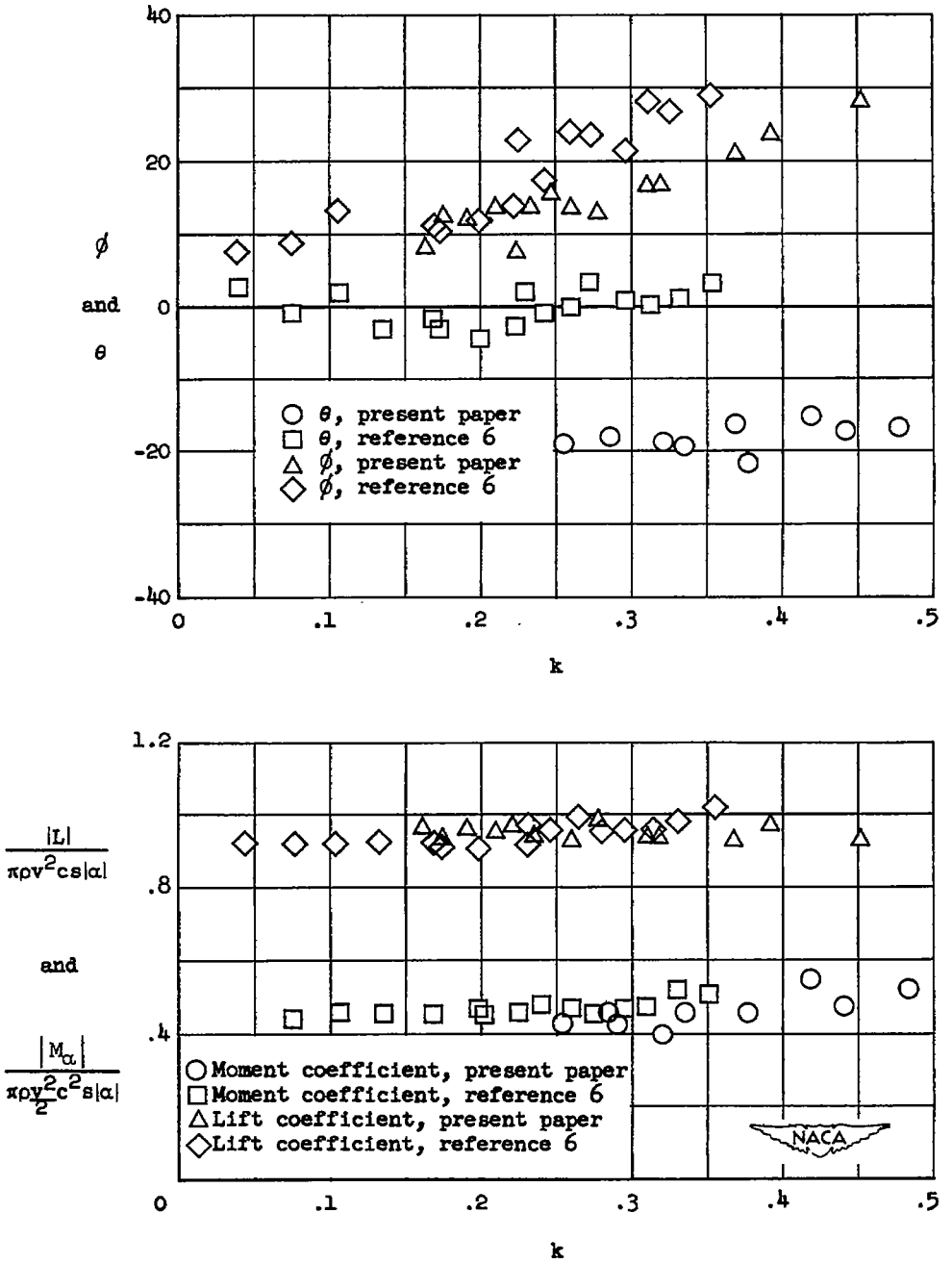

Figure 2.- Comparison of the variation of experimental aerodynamic coefficients with k of this report with the variation given in reference 6. For reference 6 data, $M \approx 0.13$ and $0.7 \times 10^6 < R < 0.88 \times 10^6$.

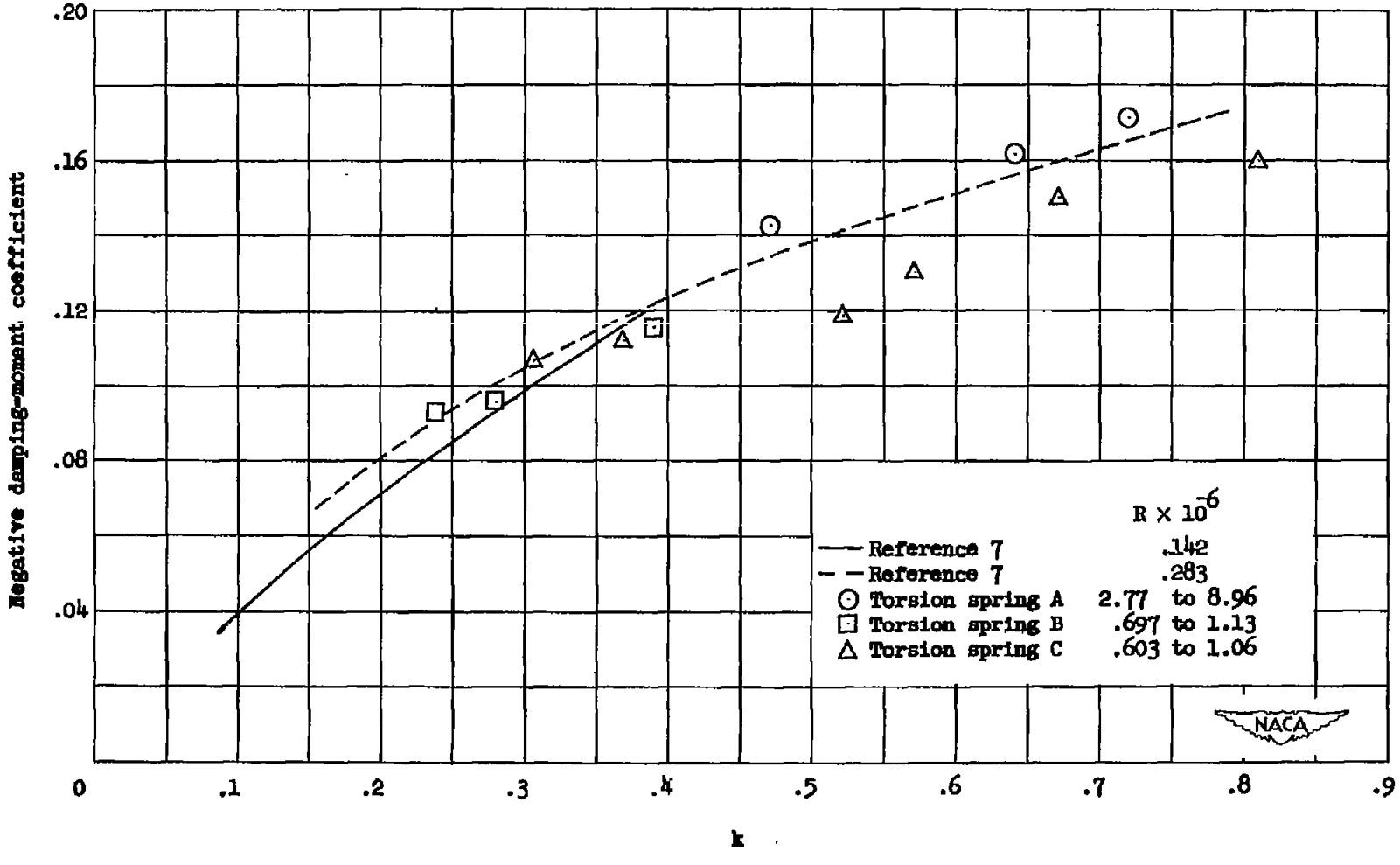

Figure 3.- Variation of experimental damping-moment coefficient with k. $M < 0.5$ for all points. A = 2.

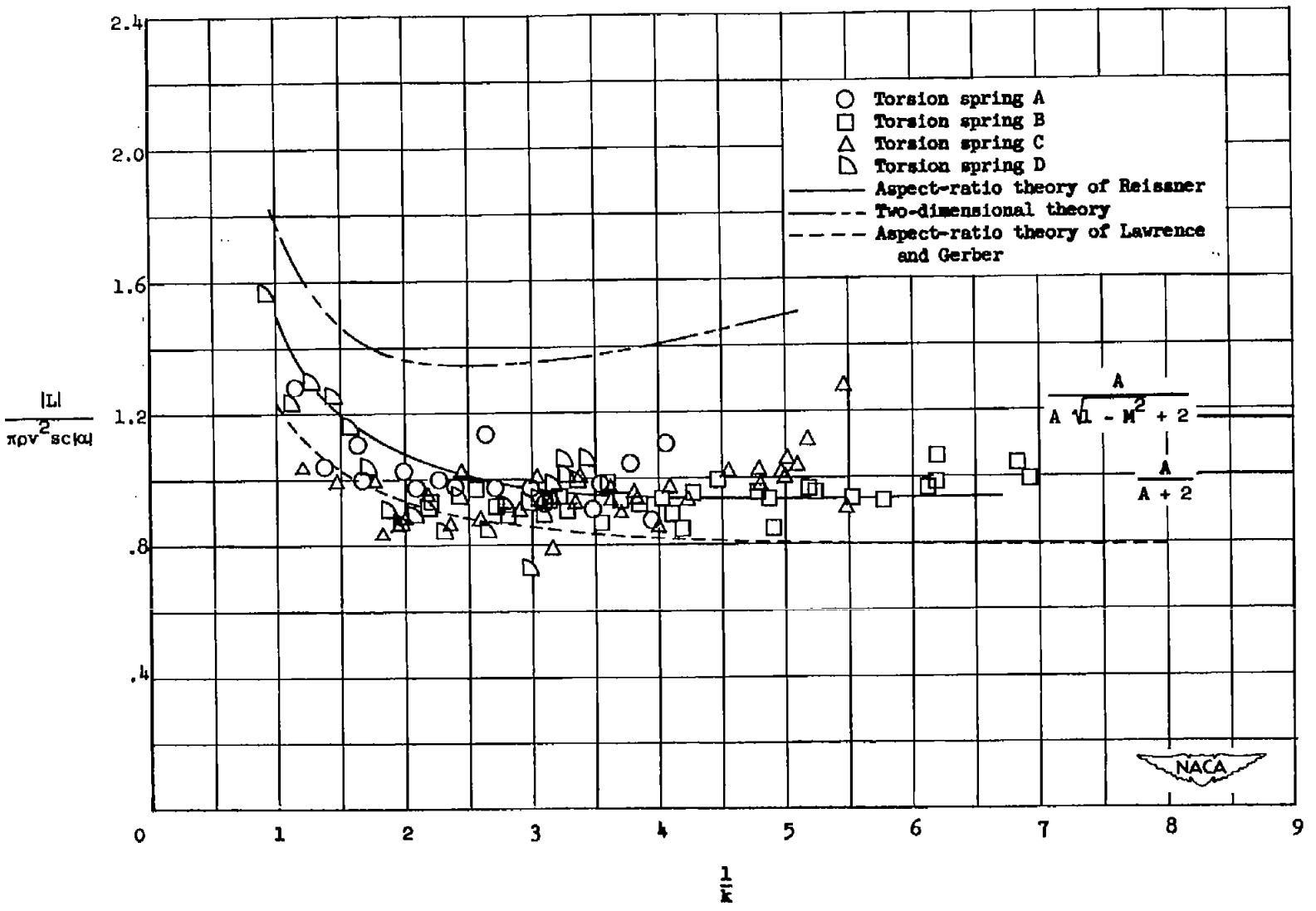

Figure 4.- Variation of theoretical and experimental lift coefficients with 1/k.

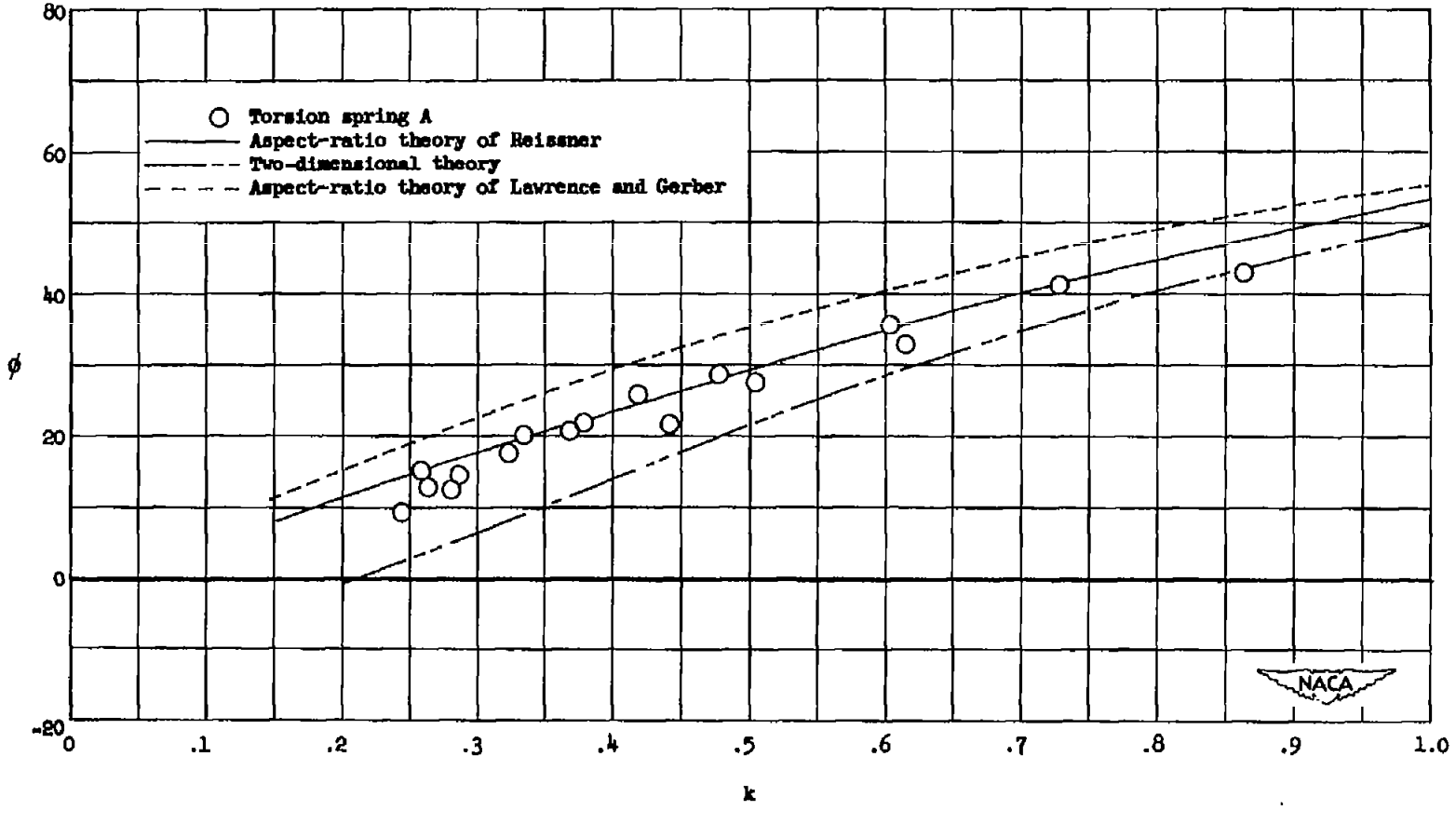

Figure 5.- Variation of theoretical and experimental lift phase angles with reduced frequency. $M \approx 0.1875(1/k)$.

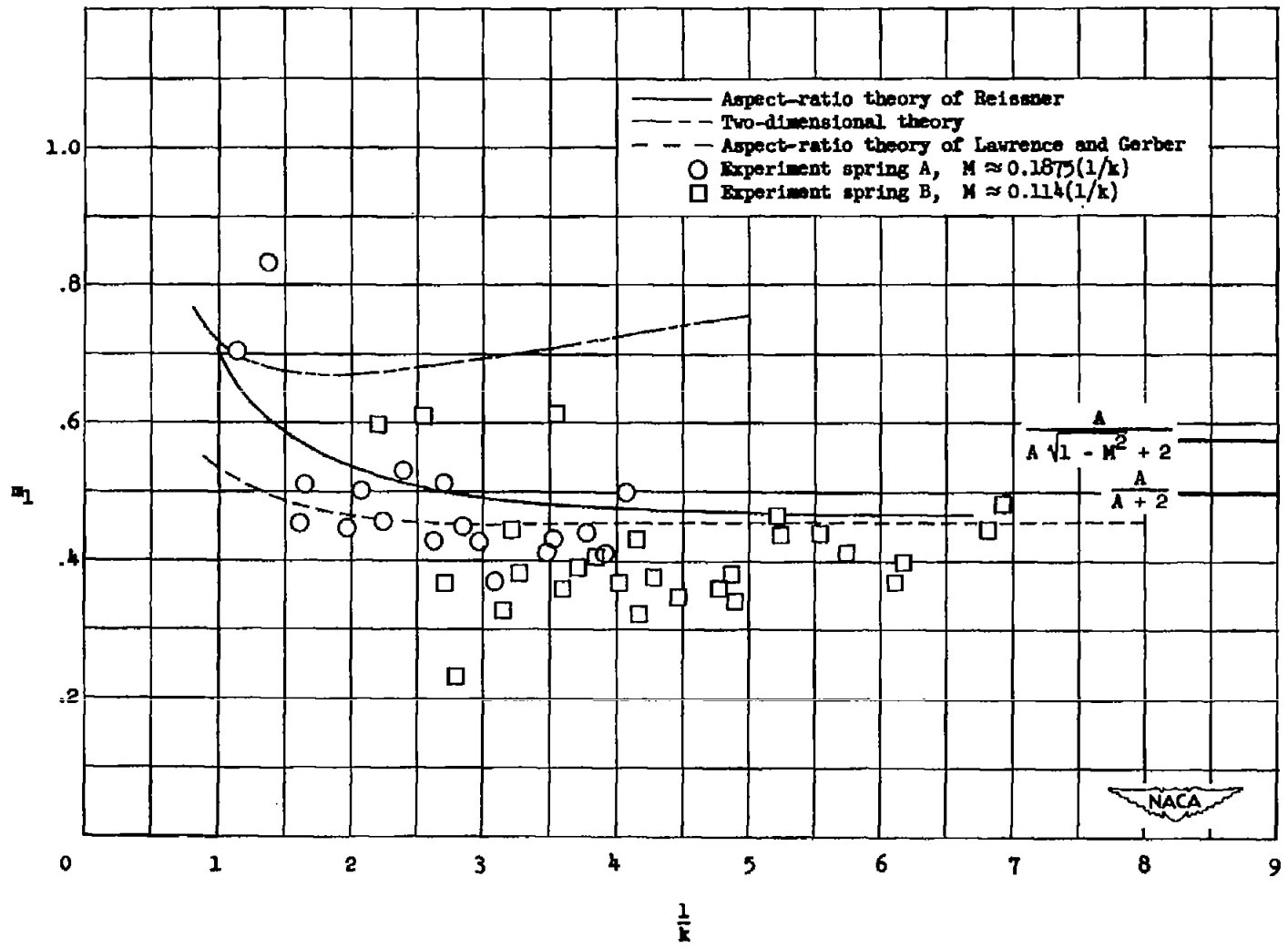

Figure 6.- Variation of theoretical and experimental in-phase moment-component coefficients with 1/k for torsional springs A and B.

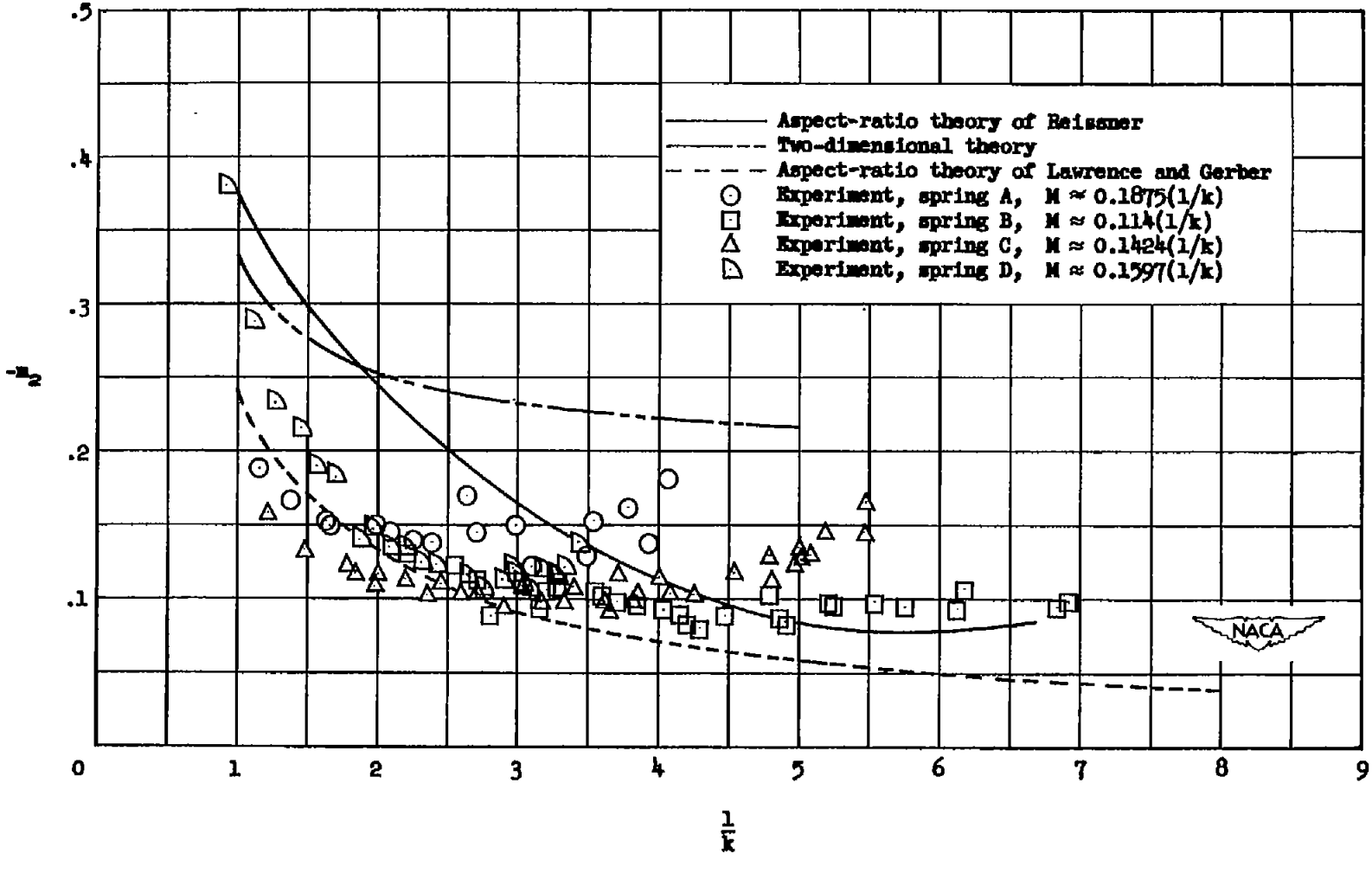

Figure 7.- Variation of theoretical and experimental damping-moment-component coefficients with l/k for torsional springs A, B, C, and D.

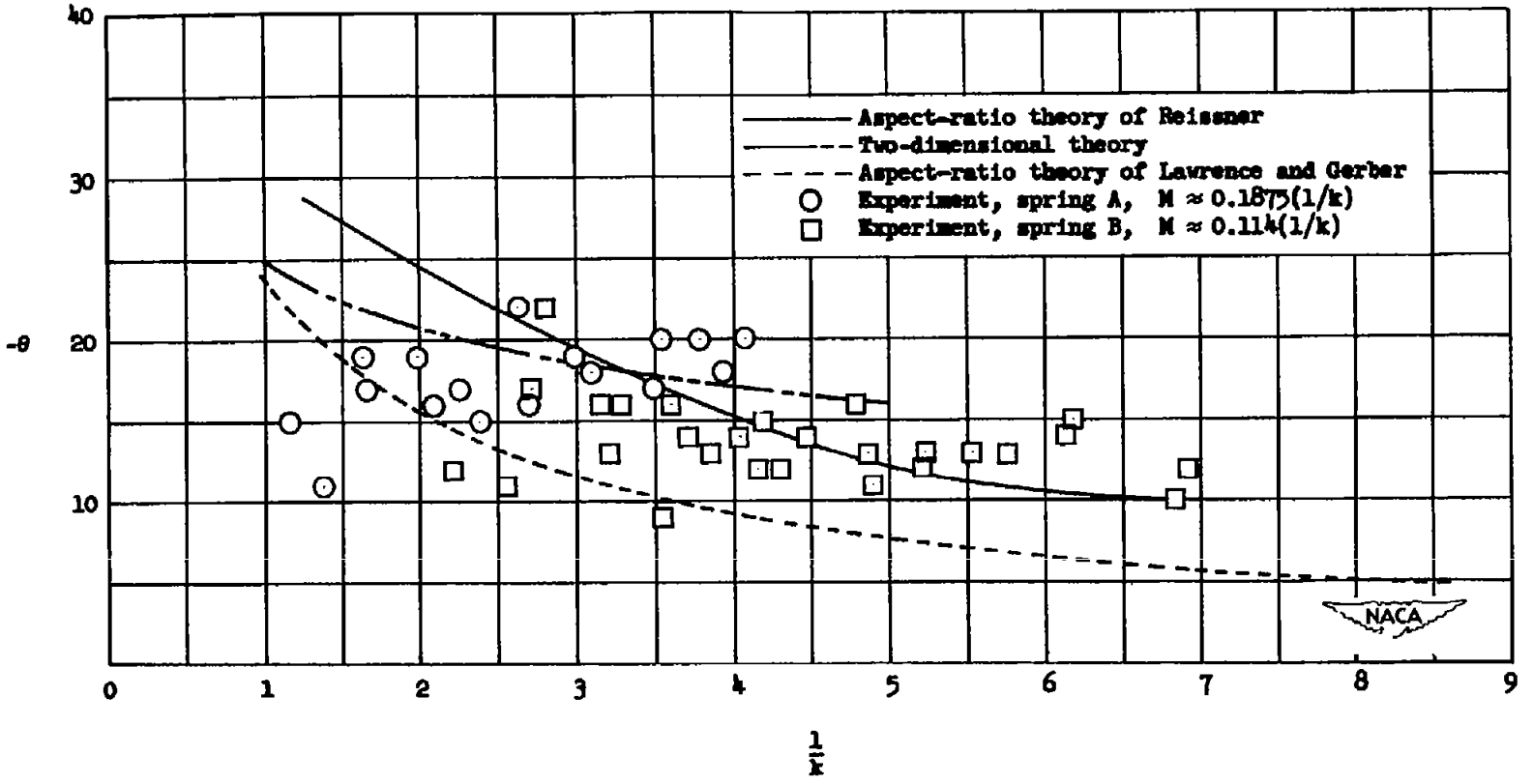

Figure 8.- Variation of theoretical and experimental moment phase angles with 1/k for torsional springs A and B.

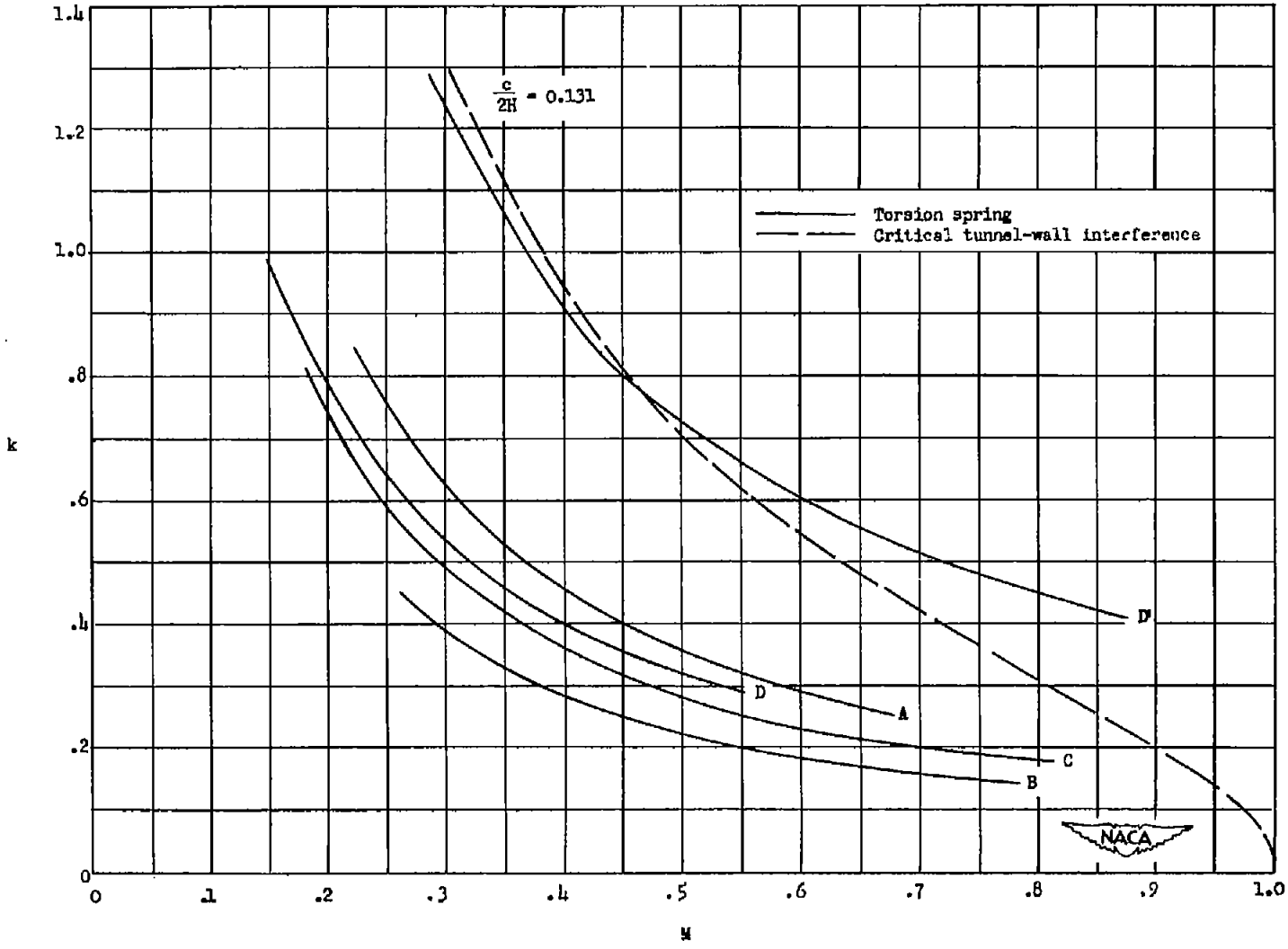

Figure 9.- Range of experimental studies indicated by variation of reduced frequency with Mach number.

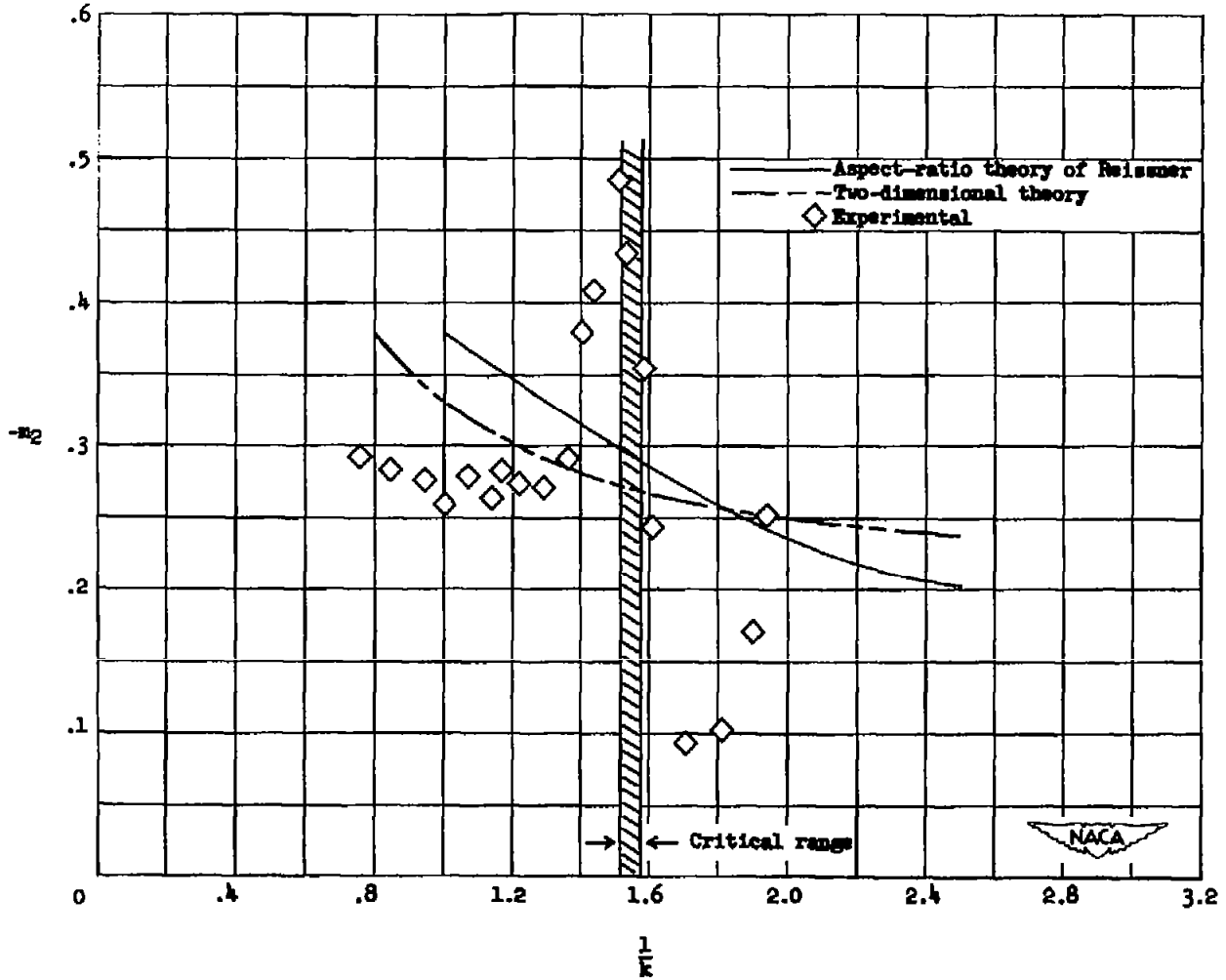

Figure 10.- Theoretical and experimental damping-moment coefficients indicating tunnel-wall effects plotted against $1/k$ for torsional spring D'. $M \approx 0.350(1/k)$.

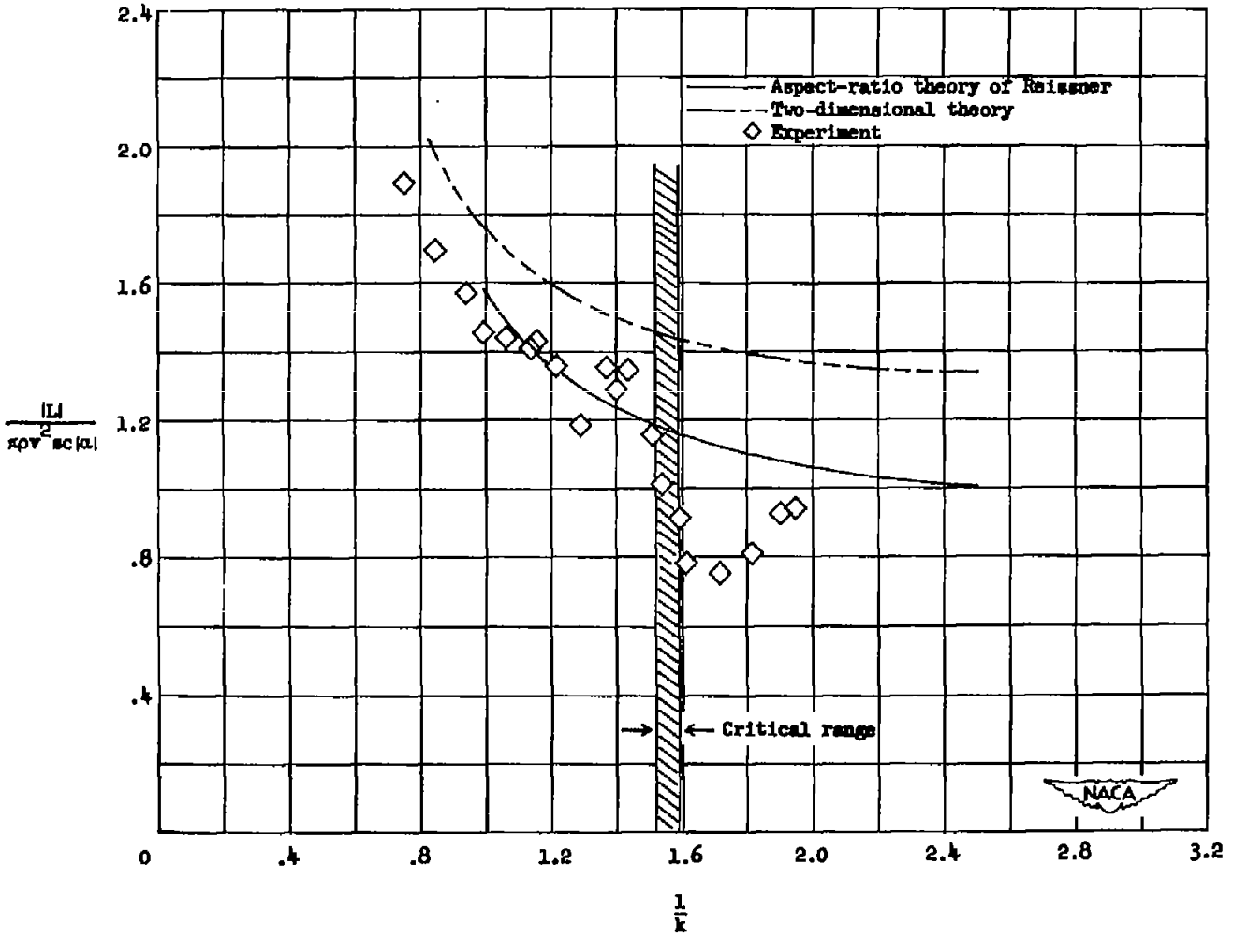

Figure 11.- Theoretical and experimental lift coefficients indicating tunnel-wall effects plotted against $1/k$ for torsional spring D'. $M \approx 0.35(1/k)$.